# 2 Gravitational wave

## 2.1 Einstein equations

The space-time that shift slightly from Minkowski metric $\eta_{ij}$ is represented as below.

$$g_{ij} = \eta_{ij} + h_{ij} \tag{1}$$

$$\eta_{ij} = \begin{pmatrix} -1 & 0 & 0 & 0 \\ 0 & 1 & 0 & 0 \\ 0 & 0 & 1 & 0 \\ 0 & 0 & 0 & 1 \end{pmatrix}$$

$$|h_{ij}(x)| \ll 1$$

($h_{ij}(x)$ is the symmetric tensor.)

Assume that each component of $h_{ij}$ is far less than 1, above second order of $h_{ij}$ is ignored. Under this approximation, contravariant metric tensor $g^{ij}$ is

$$g^{ij} = \eta^{ij} + h^{ij} \tag{2}$$

Contravariant metric tensor $\eta^{ij}$ is defined as $\eta^{ij}\eta_{jk} = \delta^i_k$.

$$\eta^{ij} = \begin{pmatrix} -1 & 0 & 0 & 0 \\ 0 & 1 & 0 & 0 \\ 0 & 0 & 1 & 0 \\ 0 & 0 & 0 & 1 \end{pmatrix}$$

Here define

$$\phi_{ij} \equiv h_{ij} - \frac{1}{2}hg_{ij} = h_{ij} - \frac{1}{2}h\eta_{ij} \tag{3}$$

$$h \equiv h^i_j = g^{ij}h_{ij} = \eta^{ij}h_{ij} \tag{4}$$

Therefore

$$h_{ij} = \phi_{ij} - \frac{1}{2}\phi\eta_{ij} \tag{5}$$

$$\phi = \phi^i_i = -h \tag{6}$$

$T_{ij}$ is stress - energy - momentum tensor. Einstein equations is

$$R_{ij} - \frac{1}{2}Rg_{ij} = \frac{8\pi G}{c^4}T_{ij} \tag{7}$$

Ricci tensor is

$$R_{ik} = \frac{1}{2}\left[\frac{\partial}{\partial x^i}\left(\frac{\partial h^j_k}{\partial x^j} - \frac{1}{2}\frac{\partial h}{\partial x^k}\right) + \frac{\partial}{\partial x^k}\left(\frac{\partial h^j_i}{\partial x^j} - \frac{1}{2}\frac{\partial h}{\partial x^l}\right) - \Box h_{ik}\right] \quad (8)$$

Scalar curvature is

$$R = \frac{\partial^2 \phi^{ij}}{\partial x^i \partial^j} - \frac{1}{2}\Box h \quad (9)$$

Therefore the Einstein equation is represented as below.

$$\Box\phi_{ij} - \frac{\partial}{\partial x^i}\left(\frac{\partial \phi^k_j}{\partial x^k}\right) - \frac{\partial}{\partial x^j}\left(\frac{\partial \phi^k_i}{\partial x^k}\right) - -\frac{\partial}{\partial x^k}\left(\frac{\partial \phi^l_m}{\partial x^l}\right)\eta^{km}_{ij} = -\frac{16\pi G}{c^4}T_{ij} (10)$$

From Gauge transformation

$$x'^i = x^i + \xi^i$$

and Gauge condition,

$$\frac{\partial \phi'^j_i}{\partial x'^j} = 0$$

The Einstein equations is rewritten by

$$\Box\phi_{ij} = -\frac{16\pi G}{c^4}T_{ij} \quad (11)$$

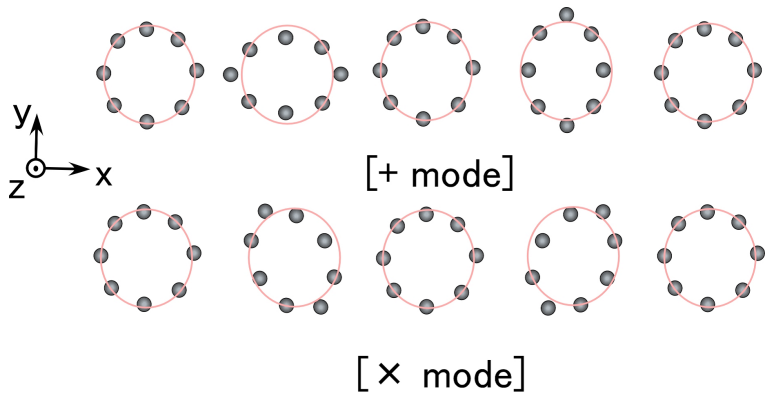


Figure 1: Gravitational wave modes

### 2.2 Plane wave propagation

Assuming the plane wave in a vacuum, the wave equation is represented as below.

$$\Box\phi_{ij} = 0$$

Solution of this equation is

$$\phi_{ij} = a_{ij} \exp ik_l x^l$$

This satisfies follow relations.

$$k_l k^l = 0$$

$k_l$ is the 4 dimension vector of gravitational wave propagation. $a_{ij}$ is the symmetric constant tensor, that stands for amplitude. By Gauge condition,

$$a_{ij} k^j = 0$$

and assuming the angular frequency $\omega$,

$$\omega = kc.$$

Under the Gauge transformation, amplitude after transformation $a'_{ij}$ by original one,

$$a'_{ij} = a_{ij} - \epsilon_i k_j - \epsilon_j k_i + \eta_{ij}\epsilon_l k_l$$

Supposing that gravitational wave is propagating $x^3$ direction. $x^0 = ct$ , $x^3 = z$ for simplifying, by optimizing the $\epsilon_i$,

$$a'_{00} = a'_{01} = a'_{02} = 0$$

and

$$a_{11}^{'} = -a_{22}^{'}$$

or

$$a_{12}^{'} = a_{21}^{'}$$

Therefore $A^{+}$, $A^{\times}$ represent each amplitude mode

$$\phi_{ij} = A^{+}e_{ij}^{+}exp(-ikx^{0} + ikx^{3}) + A^{\times}e_{ij}^{\times}exp(-ikx^{0} + ikx^{3}) \quad (12)$$

$$e_{ij}^{+} = \begin{pmatrix} 0 & 0 & 0 & 0 \\ 0 & 1 & 0 & 0 \\ 0 & 0 & -1 & 0 \\ 0 & 0 & 0 & 0 \end{pmatrix}$$

$$e_{ij}^{\times} = \begin{pmatrix} 0 & 0 & 0 & 0 \\ 0 & 0 & 1 & 0 \\ 0 & 1 & 0 & 0 \\ 0 & 0 & 0 & 0 \end{pmatrix}$$

By equation (5),

$$h_{ij} = \phi_{ij} = A^{+}e_{ij}^{+}exp(-ikx^{0} + ikx^{3}) + A^{\times}e_{ij}^{\times}exp(-ikx^{0} + ikx^{3}) \quad (13)$$

There are 2 vibration modes that are transverse wave with light speed.

### 2.3 Energy of gravitational wave

From the compensated momentum equation, the one-round time average of gravitational field energy $< t_i^j >$ is represented as follow.

$$< t_i^j >= \frac{k^2c^4}{32\pi G}(A^{+2} + A^{\times 2}) \begin{pmatrix} -1 & 0 & 0 & -1 \\ 0 & 0 & 0 & 0 \\ 0 & 0 & 0 & 0 \\ 1 & 0 & 0 & 1 \end{pmatrix}$$

Therefore the energy flow to the $x^3$ direction is

$$F^3 =< t_0^3 > c = \frac{k^2c^5}{32\pi G}(A^{+2} + A^{\times 2})$$

| Frequency [Hz] | Detector | Source |
|---|---|---|
| $\sim 10^{-16}$ | Anisotropy of microwave background | Primordial |
| $\sim 10^{-9}$ | pulsar timing | Primordial, cosmic strings |
| $\sim 10^{-4}$ to $10^{-1}$ | Doppler tracking of Space craft | binary stars, supermassive black holes |
| $\sim 10$ to $10^{3}$ | Laser interferometer | inspiral: NS+NS, BH+BH, NS+BH |
| $10^{3} \sim$ | Cryogenic resonant bar detector | supernovae, spinning neutron stars |

Table 1: The relation sources and range

| Source | Distance | Event rate (per year) |
|---|---|---|
| Binary neutron stars coalescence | $8.2 * 10^{9}$ly | 5 |
| Black holes coalescence | $65 * 10^{9}$ly | 1∼30 |
| Supernova explosion | $33 * 10^{6}$ly | 1 |
| Quasi-normal mode | $100 * 10^{9}$ly | |

Table 2: KAGRA estimation

### 2.4 Sources of gravitational wave

Gravitational wave is emitted by merging binaries, supermassive black holes and stochastic background.

1. Merging compact binary systems
   The coalescence of a compact binary system can be classified in three phase: (1) During the inspiral. (2) During merging phase. (3) After merged phase. Two neutron stars, two black holes, or one neutron star and one black hole have huge mass and are close together, they rotate rapidly. They start out by spiraling each other at some distance. When their orbital separation is on the order of kilometers, they radiate an enormous

amount of energy in a short time. They emitted gravitational waves increase in amplitude and this waveform is called a chirp. Eventually the stars will coalesce. When they have merged into a single star, the system de-excites by emitting gravitational waves. It is predicted that merging compact binary system emit gravitational wave s in the 10Hz to 1000 Hz frequency bands. It is possible to determine the distance to these objects by analyzing their waveforms.

2. Supermassive black holes
   One of the most exciting topics in astronomy concerns the mystery of why the number density of active galactic nuclei decrease with increasing redshift. A popular hypothesis is that black holes with thousands to billions of solar masses are at the center of every galaxy. Such black hole events include coalescences, collapses of individual such black holes and gravitational slingshots. By measuring such events it might be determine such black hole masses, mechanism by which they form, their rate of formation, and the rate at which they coalesce or collapse.

3. Stochastic background
   Just as density fluctuation in the early universe resulted in the anisotropic cosmic microwave background, so might these initial perturbations have caused a stochastic background of gravitational waves. The most important difference between the stochastic background and the cosmic microwave background is that, since they couple so weekly to matter, gravitational waves did not thermalize. Thus, the gravitational wave spectrum should come to us unaltered from whatever produced it. If it is possible to detect the stochastic background, it would be able to make inferences about a much earlier universe than we have been able to do with electromagnetic radiation.

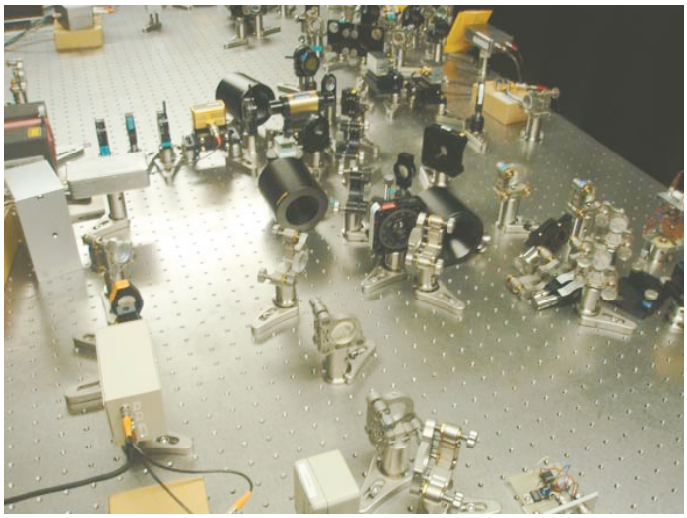

Figure 2: Fabry Perot cavity lock system for verification mirror mounts stability. Cavity could be locked with 20m radius of mirror curvature against the 10cm cavity.

# 3 Interferometer

Gravitational wave is tidal distortion. The ways to detect of gravitational wave are the pulsar timing by observe the interval of pulse, resonant bar, which uses the elasticity of material, and interferometer. Now the most developing method is the interferometer. This interferometer is basically Michelson interferometer. Michelson interferometer has two perpendicular arms. The distortion could be the phase variations of laser and these two beams from those arms could be interfered each other in detection port of interferometer. This variation is only $10^{-21}$m in ground detector. Therefore there are some techniques for high sensitivity of interferometer. For instance the longer arm could detect with the higher sensitivity. The possible frequency of gravitational wave is restricted by some parameters. Space antenna is another option for lower range by 1000km arm length.

In this section, interferometer principle and related things are introduced.

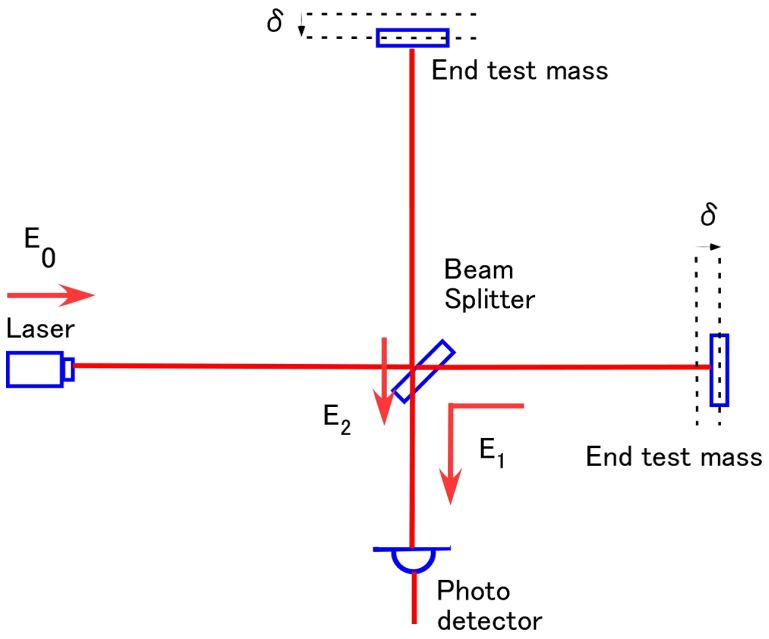


Figure 3: Detection by michelson interferometer

### 3.1 Detection of space-time distortion by laser

The end test mass displacement by $\delta = a \sin \omega t$ could be the phase modulation shown below. $E_0$ is input field and $E_1, E_2$ is inline and perpendicular field at antisymmetric port. Assume in this calculation that the power reflectivity and transmittance of beam splitter are 0.5 each.

$$\begin{aligned} E_1(t) &= \frac{tr}{2} E_0 e^{i\frac{2L+2\delta}{c}\Omega} \\ E_2(t) &= \frac{rt}{2} E_0 e^{i\frac{2L-2\delta}{c}\Omega} \end{aligned} \tag{14}$$

$\Delta$ is the phase change by end mirror displacement.

$$\begin{aligned} \Delta &= 2\pi \frac{c}{\lambda} \frac{2a \sin \omega t}{c} \\ &= 2\pi 2 \frac{a}{\lambda} \sin \omega t \end{aligned}$$

$$i\Delta = \frac{4\pi}{2}\frac{a}{\lambda}(e^{i\omega t} - e^{-i\omega t})$$

$$\begin{aligned}
E_1(t) &= \frac{tr}{2}E_0 e^{i\frac{2L}{c}\Omega}e^{i\frac{2\delta}{c}\Omega} \\
&= \frac{tr}{2}E_0 e^{i\frac{2L}{c}\Omega}(1+i\Delta) \qquad (15) \\
E_2(t) &= \frac{tr}{2}E_0 e^{i\frac{2L}{c}\Omega}e^{i\frac{2\delta}{c}\Omega} \\
&= \frac{tr}{2}E_0 e^{i\frac{2L}{c}\Omega}(1-i\Delta) \qquad (16) \\
& \qquad (17)
\end{aligned}$$

$$\begin{aligned}
E_2(t) &= \frac{tr}{2}E_0 e^{i\frac{2L}{c}\Omega}\left(1 - 2\pi\frac{a}{\lambda}(e^{i\omega t} - e^{-i\omega t})\right) \\
&= E_2^0 + E_2^+ + E_2^- \qquad (18) \\
E_2^0 &= \frac{tr}{2}E_0 e^{i\frac{2L}{c}\Omega} \\
E_2^+ &= -\frac{2\pi a}{\lambda}\frac{tr}{2}E_0 e^{i\frac{2L}{c}\Omega}e^{i(\Omega+\omega)t} \\
E_2^- &= +\frac{2\pi a}{\lambda}\frac{tr}{2}E_0 e^{i\frac{2L}{c}\Omega}e^{i(\Omega-\omega)t}
\end{aligned}$$

This is the effect of modulation $\omega$ by displacement. Seeing above equations, the tidal distortion by gravitational wave could be the phase modulation. The interferometer like Michelson interferometer that has orthogonal lines for light traveling could rightly detect those phase as fringe at the detection port.

If the detection port is set by dark fringe, the sum of those light is as follow. Assume in this calculation that the power reflectivity and transmittance of beam splitter is 0.5 each.

$$\begin{aligned}
|E_1 - E_2| &= 2|E_2^+ + E_2^-| \\
&= \left(\frac{2\pi a}{\lambda}\frac{tr}{2}E_0 e^{i(\Omega+\omega)t} - \frac{2\pi a}{\lambda}\frac{tr}{2}E_0 e^{i(\Omega-\omega)t}\right) \\
&= \left(\frac{2\pi a}{\lambda}\frac{rt}{2}E_0 e^{i\Omega t} * [e^{i\omega t} - e^{-i\omega t}]\right) \\
|E_1 - E_2|^2 &\propto |E_0|^2 (1 + \cos 2\omega t) \qquad (19)
\end{aligned}$$

On the other hand, laser phase $\phi$ after traveling one round through the arm has been changed by

$$\int_{t-\frac{2L}{c}}^{t} \frac{1}{2} h(t') c dt' = \frac{hc}{\Omega_{GW}} \sin \frac{L\Omega_{GW}}{c} \sin \left( \Omega_{GW} t - \frac{L\Omega_{GW}}{c} \right) \tag{20}$$

When

$$\frac{L\Omega_{GW}}{c} \ll \frac{\pi}{2},$$

$\delta$ L is the differential distance by gravitational wave and that is

$$\delta L \sim L \times h. \tag{21}$$

$$\tag{22}$$

$\phi$ is phase and that is

$$\phi = 2\pi \times \frac{2\delta L}{\lambda}. \tag{23}$$

Therefore the distance change effect by gravitational wave is converted to laser phase, and then the signal is detected as the fringe.

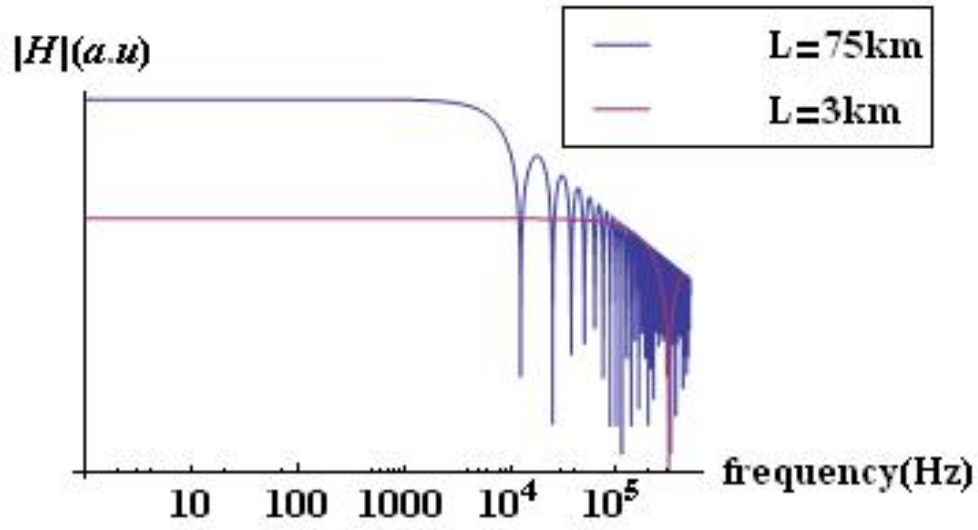


Figure 4: Michelson interferometer sensitivity

### 3.2 Michelson Interferometer

Michelson interferometer (MI) is the simple interferometer for gravitational wave detector. The arm length is defined as distance from beam splitter to the each end test mass. This arm length determine the detectable gravitational wave frequency $f_{GW}$ by Michelson interferometer.

$$f_{GW} = \frac{c}{4L} \tag{24}$$

The phase shift being accumulated in the arm at the higher frequency, the laser interferometer sensitivity is degraded. Figure4 shows comparison by arm length.

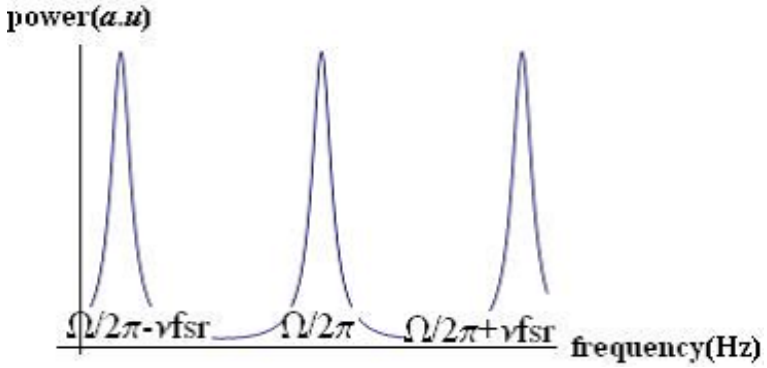


Figure 5: Free spectral range

### 3.3 Fabry Perot cavity

Fabry Perot Michelson interferometer (FPMI) is the MI with Fabry Perot (FP) cavity in each arm. This system is equivalent to lengthened arm. Each FP cavity is composed of 2 mirrors whose reflective surfaces confront. Laser beam travels several rounds at the FP cavity according to the finesse F.

**Free spectral range** Cavity could amplify particular frequency light. And the light could be transmitting through the cavity. In frequency range, there is the periodic maximum transmitted power from the cavity. This period is called as the free spectral range (FSR). This FSR ($\nu_{FSR}$) is written as follow using the cavity length L.

$$\nu_{FSR} = \frac{c}{2L}$$

**Cavity finesse** Cavity finesse F is defined as the sharpness of resonance of cavity. This is defined by $\nu_{FSR}$ and $\nu_{FWHM}$. $\nu_{FSR}$, which is the one cycle frequency that is maximizing transmitted power, what is called free spectral range (FSR), and $\nu_{FWHM}$ is the full width at half maximum. Therefore that is notated by input test mass and end test mass amplitude reflectivity ($r_1$, $r_2$). F is as follow.

$$F = \frac{\nu_{FSR}}{\nu_{FWHM}} = \frac{\pi\sqrt{r_1 r_2}}{1 - r_1 r_2} \tag{25}$$

Finesse is depending only on reflectivity of mirrors composing cavity.

**Stability of cavity** The cavity stability especially about longitudinal mode determine by the radius curvature of mirrors that are constructing the cavity. This parameter is g-factor. g-factor is

$$g = 1 - \frac{L}{R}.$$

And the condition of cavity stable is $0 \leq g_1 * g_2 \leq 1$. $g_1, g_2$ are the g-factor of input mirror and end mirror each.

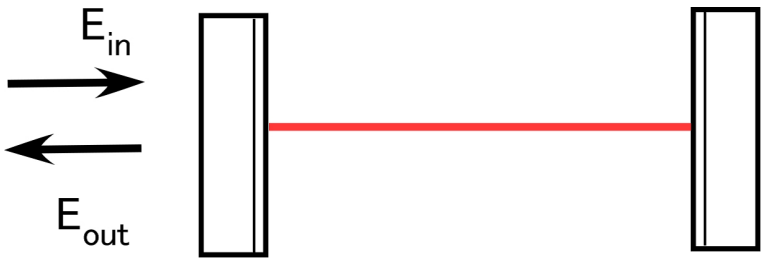


Figure 6: FP cavity transfer function

**Cavity response** Assuming that $T_1, t_1$, which is the intensity and amplitude transmittance of input test mass each (therefore $T_1 = t_1^2$) and $\phi$, which is the phase shift in the FP cavity, the cavity response is calculated as below.

$$\begin{aligned}
\left|\frac{E_{out}}{E_{in}}\right|^2 &= \left|\frac{t_1}{1 - r_1 r_2 e^{i\phi}}\right|^2 \\
&= \left|\frac{t_1}{1 - r_1 r_2 (1 + i\phi)}\right|^2 \\
&= \left|\frac{t_1^2}{(1 - r_1 r_2)^2 + (r_1 r_2)^2 \phi^2}\right| \\
&= \frac{t_1^2}{\left(\frac{T_1}{2}\right)^2 + \phi^2} \\
&= \frac{T_1 / \left(\frac{T_1}{2}\right)^2}{1 + \left(\frac{2}{T_1}\right)^2 \phi^2} \\
&= \frac{4}{T_1} \frac{1}{1 + \left(\frac{2}{T_1}\phi\right)^2}
\end{aligned} \tag{26}$$

Maximum power in cavity is $\frac{4}{T_1}$.

$$\begin{aligned}
\left|\frac{P_{out}}{P_{in}}\right| &= \frac{4}{T_1} \frac{1}{1 + \left(\frac{2}{T_1} 2\pi \frac{2\delta}{\lambda}\right)^2} \\
&= \frac{4}{T_1} \frac{1}{1 + \left(2\pi \frac{\delta}{\Delta}\right)^2}
\end{aligned} \tag{27}$$

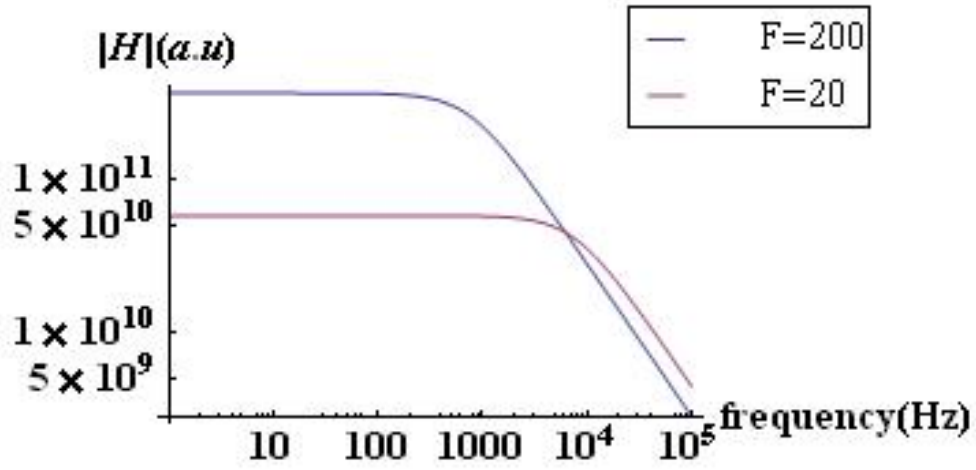


Figure 7: FP cavity transfer function

$$\Delta = \frac{T_1}{4}\lambda \tag{28}$$

$\delta$ is difined as distance. $\Delta$ is the decay of power in cavity.

**Cavity pole** Furthermore cavity pole $\gamma$, which is cut-off frequency of detector, is

$$\gamma = \frac{T_1 c}{4L}. \tag{29}$$

The figure shows that floor level is proportional to the finesse, while cavity pole is inverse proportional to finesse. At lower range, high finesse has good sensitivity and narrow band. Lower finesse cavity has wider band and good sensitivity at higher range.

**Reflectivity of cavity** The front mirror reflectivity and transmittance are $'r_1'$, $'t_1'$ and end mirror are $'r_2'$, $'t_2'$. The cavity reflectivity R is represented as follow.

$$R = -r_1 + \frac{t_1^2 r_2 e^{i\phi}}{1 - r_1 r_2 e^{i\phi}} \tag{30}$$

This value is changeable according to the cavity resonance condition. If the cavity is on resonant, the reflectivity of cavity $R_{res}$ is

$$R_{res} = \frac{-r_1 + r_2}{1 - r_1 r_2}.$$

On the other hand, if anti-resonant, the reflectivity of cavity $R_{anti}$ is

$$R_{anti} = -\frac{r_1 + r_2}{1 + r_1 r_2}.$$

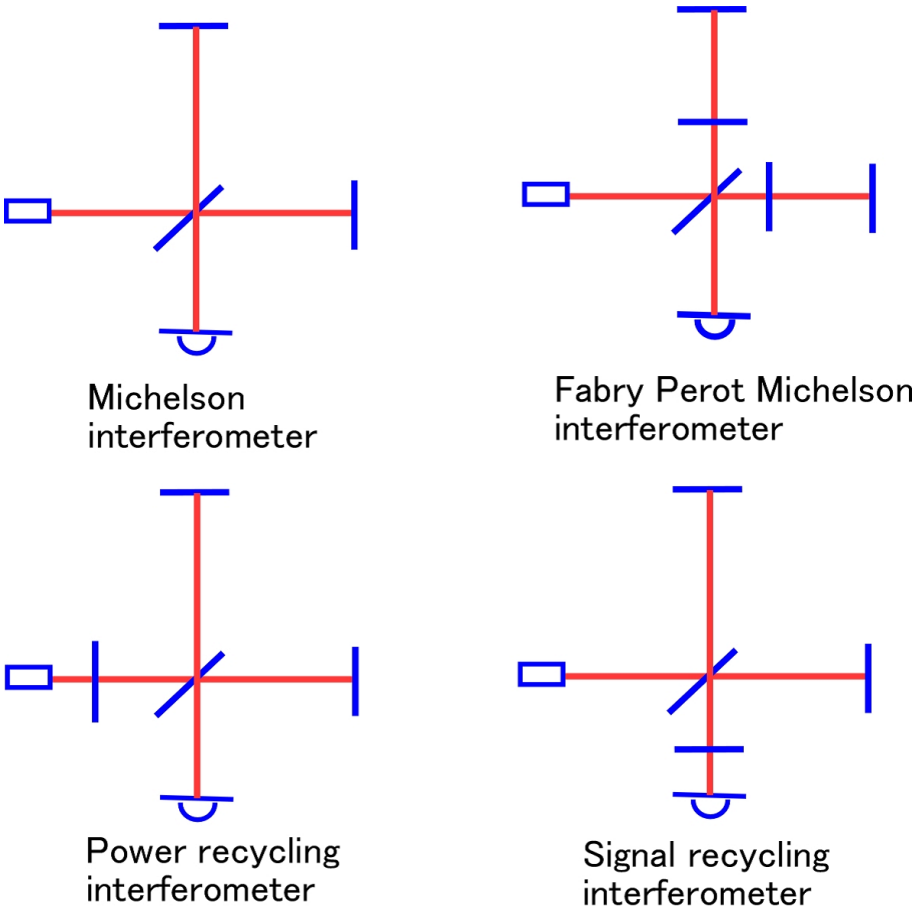


Figure 8: various IFO types

### 3.4 Various interferometers

There are some combinations of interferometer. Each type has own properties.

- Long arm length is for broad band sensitivity.
  Fabry Perot cavity in the arms makes it possible to effective distance to travel the gravitational wave. Finesse is the indication of number of recycling in the arm. This finesse is defined by arms reflectivity. High finesse cavity is more amplify the gravitational wave signal while the linear range for the control of length is narrower.

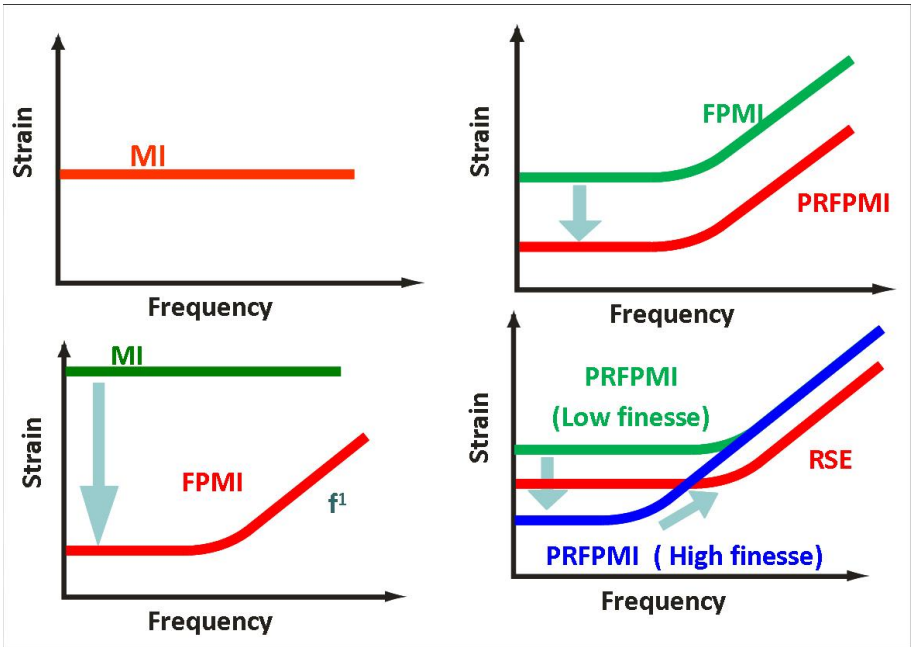


Figure 9: Comparison of shot noise

Interferometer types → FPMI, PRFPMI, RSE.

- High power laser reduces shot noise.
  The reflected field goes directly to symmetric port, and was disposed before. Instead of wasting this power, put the additional mirror at symmetric port in front of the laser. This mirror works as the power recycling. Power recycling gain $G_{PRM}$is defined by interferometer total loss $L_{loss}$.

$$G_{PRM} = \frac{1}{L_{loss}}$$

  Interferometer types →PRMI, PRFPMI, RSE

- Signal amplification to optimize shot noise.
  Signal extraction mirror at anti-symmetric port make the gravitational wave signal extract before the cancellation in the high finesse arm cavity. This mirror make the signal extraction cavity finesse lower, then the signal could be obtained while am-

plified by arm cavity.
Interferometer types →Dual Recycling, RSE

Figure9 shows those interferometer comparison in the point of shot noise.
The shot noise is white noise in the Michelson interferometer. If applied the Fabry Perot cavity in the arm, this shot noise decreases at DC by increasing power in arm and increase at high frequency by signal phase is cancelled.
Adding power recycling mirror makes it possible to reuse the power back to the laser, therefore the shot noise is suppressed.
Comparing to the high finesse power recycling MI and low finesse one, the shot noise at DC is decreased by the finesse. And RSE interferometer seeing the later caption, which could make the arm cavity finesse high and low finesse power recycling for thermal noise, can make shot noise lower than low finesse power recycling FPMI at high frequency, higher than high finesse power recycling FPMI at DC though.
As this principle, RSE is optimized to the shot noise and could detect the neutron stars coalescence in $6.2 * 10^9$ly.

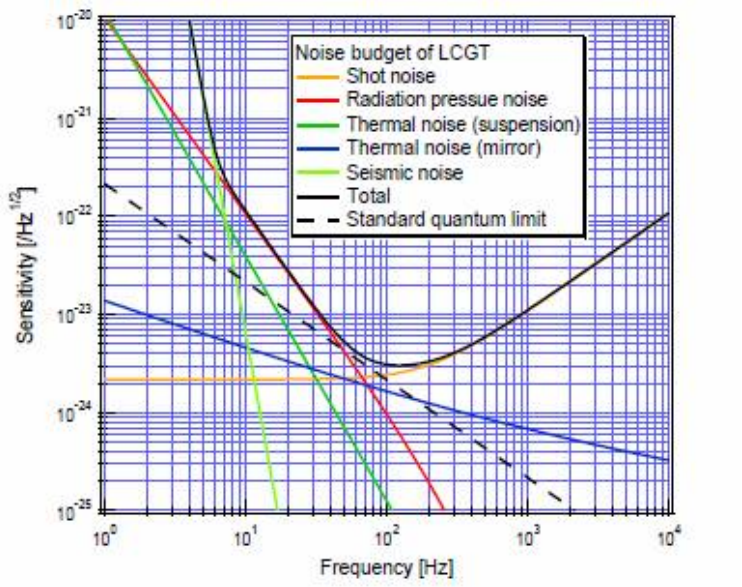


Figure 10: KAGRA design sensitivity and noise budget

### 3.5 Sensitivity

The sensitivity of detector is limited various noises. There are seismic noise, radiation pressure noise, thermal noise, violin modes, and shot noise. For instance, Figure10 is the KAGRA sensitivity.

- Seismic noise
  Suspended mirror displacement $z(f)$ by seismic motion is written in follow. $m$ is the mass, $z$ is the position of mass, $l$ is the suspension length and $s(t)$ is the displacement of suspension point.

$$\begin{aligned} mg\frac{z-s(t)}{l} &= -m\ddot{z} \\ \frac{g}{l}\left(z(f)-s(f)\right) &= f^2 z(f) \\ z(f) = \frac{-f_0^2}{f^2-f_0^2}s(f) f_0 &= \sqrt{\frac{g}{l}} \end{aligned} \tag{31}$$

  s(f) is the unique parameter depending on the local seismic

motion. For KAGRA, $s(f) = 10^{-9}$.

- Thermal noise
  Heat bath gives the energy to the materials in the interferometer and gives them noise. This thermal noise has two kinds of categories, which are suspension thermal noise and mirror thermal noise.

  – Suspension thermal noise
    Thermal noise causes the fluctuations of the center of gravity of mirror. This is suspension thermal noise ($S_s$).

$$S_s = \frac{4k_BT(2\pi f_{pen})}{m\Omega^5}\phi_{pen} \tag{32}$$

  – Mirror thermal noise
    Thermal noise causes the mirror surface fluctuations by thermal excitation of mirror elastic vibration. This is suspension thermal noise ($S_m$)

$$S_m = \frac{4k_BT}{\Omega}\frac{1-\nu^2}{\sqrt{\pi}Y\omega_0}\phi \tag{33}$$

    Y is young modules, $\nu$ is Poisson's ratio and $\phi$ is the mechanical loss. These equations are from fluctuation dissipation theorem,

$$S_x = \frac{8k_BTW}{\Omega^2F_0^2} \tag{34}$$

    W is dissipation by force $F_0$.

- Quantum noise
  Quantum noise is originated from the laser light composing of photon. Radiation pressure noise, which is originated from that photon give the energy to mirror, and shot noise, which is originated from photon counting statistic error at photo detector, is categorized as quantum noise. [1]

– Radiation pressure noise
  Photon energy is $\hbar\nu$. It gives its momentum to the mirror. This cause the excitation of mirror.

– Shot noise
  There are statistic frequency depended noise according to the photon counting.

In total, there is the standard quantum limit (SQL) that can not be beaten. This SQL required from uncertainty principle is follow.

$$h_{SQL}^2 \geq \frac{8\hbar}{m\Omega^2 L^2} \tag{35}$$

$$\kappa = \frac{(I_0/I_{SQL})2 * \gamma^4}{\Omega^2(\gamma^2 + \Omega^2)} \tag{36}$$

$$S_h = \frac{h_{SQL}^2}{2}(\frac{1}{\kappa} + \kappa) \tag{37}$$

$$I_{SQL} = \frac{mL^2\gamma^4}{4\Omega} \tag{38}$$

$\kappa$ is the opto-mechanical coupling constant. $\kappa(\Omega = \gamma) = 1$ minimazes $S_h$ From these equations, the shot noise and radiation pressure noise could be gained. When $\omega \ll \gamma$, the shot noise is

$$\sqrt{S_{sh}} \approx \sqrt{\frac{\hbar\Omega}{2\omega_0 I_0}}. \tag{39}$$

When $\omega \gg \gamma$, the radiation pressure noise is

$$\sqrt{S_{rd}} \approx \frac{8}{mL^2\gamma\Omega^2}\sqrt{\frac{\hbar\omega_0 I_0}{2}}. \tag{40}$$

Each noise should be eliminated by some technique. For instance, reducing the seismic motion, mirrors are suspended and detector itself of course is built in quiet place. Reducing thermal noise, mirror is cooled to 20K. Because those are originated from photons, if the laser power were increased, shot noise would be reduced. On the other hand radiation pressure noise would become larger. Therefore squeezing light for shot

noise, or heavier test mass for radiation pressure noise are ones of good selection to solve.

For instance the test mass of DECIGO, which is the space antenna of Japan, is expected 100kg while that of KAGRA is 30kg.

| | detector | country | arm length | IFO type | start from |
|---|---|---|---|---|---|
| 1st G | TAMA300 | Japan | 300m | FPMI | 1999 |
| | LIGO | U.S. | 4km(2sites) | FPMI | 2002 |
| | VIRGO | Italy, France | 3km | PRFPMI | 2003 |
| | GEO600 | Germany England | 600m | Dual Recycling | 2002 |
| 2nd G | KAGRA | Japan | 3km | RSE | 2014 |
| | adLIGO | U.S. | 4km | DRSE | 2014 |
| | LIGO-Australia | Australia | 80m | RSE | 2017 |
| 3rd G | DECIGO | Japan | 1000km | $*1$ | |
| | LISA | Europe U.S. | 50Gm | $*2$ | |
| | E.T. | Europe | 10km | $*3$ | |

Table 3: Detectors list; $*1$: FP cavities with drag free system, $*2$: Spacecraft Doppler tracking, $*3$:triangle of three L-shaped detectors

### 3.6 World activities

Laser interferometers for gravitational wave detector are spread in the world. In Japan, TAMA300 is already working, KAGRA is the under ground cryogenic detector, which it is soon to begin being built. DECIGO (DECI-hertz Gravitational wave Observatory) is the Japanese space craft detector. LIGO (Laser Interferometer of Gravitational wave Observatory: Hanford site and Louisiana site) are the United State detector, and also they have future developed detector plan, advanced LIGO and space craft plan LISA (Laser Interferometer Space Antenna). GEO600 is the Germany and England detector, VIRGO is the Italy and France one. In Europe, there is union ground detector plan, E.T (Einstein Telescope). AIGO (Australian International Gravitational Observatory) is the Australian plan.

The coincidence analyze is necessary for gravitational source identification.